PROPELLER BLADE ELEMENT MOMENTUM THEORY WITH VORTEX WAKE DEFLECTION

M. K. Rwigema
School of Mechanical, Industrial and Aeronautical Engineering
University of the Witwatersrand, Private Bag 3, Johannesburg, 2050, South Africa

Keywords: *Blade Element Momentum, Propeller, Vortex Wake, Wake Deflection*

Abstract

Various propeller theories are treated in developing a model that analyses the aerodynamic performance of an aircraft propeller along with the construct and behaviour of the resultant slip-stream. Blade element momentum theory is used as a low-order aerodynamic model of the propeller and is coupled with a vortex wake representation of the slip-stream to relate the vorticity distributed throughout the slip-stream to the propeller forces.

Nomenclature

a	axial induction factor
a'	tangential induction factor
c	chord length (m)
C_D	drag coefficient
C_l	lift coefficient
C_T	thrust coefficient
dr	blade element and annulus width (m)
dQ	torque of element or annulus (Nm)
dT	thrust of element or annulus (Nm)
F	combined tip- and hub-loss coefficient
I	momentum of inertia
N	in-plane normal force (N)
p	pressure (P)
r	radial position (m)
R	propeller radius (m)
R_{hub}	hub radius (m)
S	propeller disk/cross-sectional slip-stream area (m^2)
t	time (s)
U	resultant velocity at blade element (m/s)
V	flow velocity (m/s)
x	thrust axis location downstream from propeller (m)
α	local angle of attack (rad)
β	local element pitch angle (rad)
γ	strength of distributed annular vorticity (m/s)
γ_s	strength of distributed swirl vorticity (m/s)
Γ	strength of bound vorticity on propeller (m^2/s) blade
ϕ	angular coordinate around propeller disk (rad)
φ	local inflow angle (rad)
σ'	local solidity
ρ	air density (kg/m^3)
Ω	propeller rotational speed (rad/s)

Subscripts:

∞	free-stream
x	at station x
p	propeller/aircraft body
s	fully-developed slip-stream
0	at $\phi = \pi/2$
F	between thrust line and direction of resultant propeller force

1 Introduction

An understanding of the propeller slipstream is important in the design phase of propeller-driven aircraft. Aerodynamic performance, aircraft stability, and noise and vibration can be significantly affected by it's interactions with

structural and aerodynamic control surfaces. During the early stages of design, one of the inputs is the thrust curve of the power plant - available thrust versus flight velocity. The iterative optimisation procedure requires rapid analysis of prospective engines and propellers to compare aircraft performance and discover configuration characteristics.

A propeller producing thrust by forcing air behind the aircraft produces a slip-stream. This may rudimentarily be considered as a cylindrical tube of spiraling air propagating rearward over the fuselage and wings – having detrimental and beneficial effects. Flow within the slip-stream is faster than free-stream flow resulting in increased drag over the parts exposed to it's trajectory. The rotary motion of the slip-stream also causes the air to strike the tailplane at indirect angles, having an effect of the stability and control of the aircraft.

This analysis shows compatibility between different approaches to propeller modeling using blade element theory to predict the propeller forces, momentum theory to relate the flow momentum at the propeller to that of the far wake, and a vortical wake model to describe the slipstream deflection.

2 Mathematical Models

2.1 Momentum Theory

Classical momentum theory, introduced by Froude [1] as a continuation of the work of Rankine [2], imposes five simplifying assumptions. The flow is assumed to be: 1) inviscid, 2) incompressible, and 3) irrotational; and both 4) the velocity and 5) the static pressure are uniform over each cross section of the disk and stream-tube.

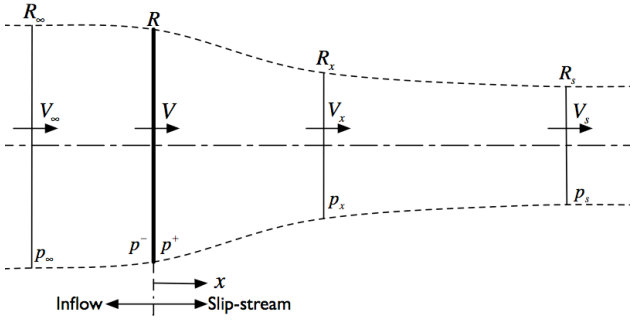

Fig. 1: Propeller stream-tube

For the axial direction, the change in flow momentum along a stream-tube starting upstream, passing through the propeller, and then moving off into the slip-stream must equal the thrust produced by this propeller, [3]

$$T = \rho\pi R_s^2 V_s (V_s - V_\infty) \qquad (1.1)$$

Applying the conservation of mass to the stream-tube control volume yields,

$$A_\infty V_\infty = AV = A_s V_s \qquad (1.2)$$

Far upstream the static pressure is p_∞ and the velocity V_∞. The static pressure falls to a value p^- immediately upstream of the actuator disk and rises discontinuously through the disk, to a value p^+ immediately downstream, although the velocity remains constant at V between these two planes, which are an infinitesimal distance apart. The thrust is therefore given by,

$$T = (p^+ - p^-)A \qquad (1.3)$$

Since the flow is inviscid, the total pressure - in accordance with Bernoulli's equation - is constant along any streamline, except for those that pass through the disk. The axial and tangential velocities are continuous as no fluid is created within the disk; the increase in total pressure is therefore experienced as an increase in static pressure. Applying Bernoulli's equation upstream and downstream of the actuator disk,

$$p^+ - p^- = \frac{1}{2}\rho(V_s^2 - V_\infty^2) \qquad (1.4)$$

From the equations above it can be shown that the velocity of the flow through the actuator disk is the average of the upstream and downstream velocities.

$$V = \frac{V_\infty + V_s}{2} \qquad (1.5)$$

An axial induction factor, a, is customarily defined as,

$$V = V_\infty(1+a) \tag{1.6}$$

and from Equation (1.5),

$$V_s = V_\infty(1+2a) \tag{1.7}$$

A real propeller, however, is never uniformly loaded as assumed by the Rankine-Froude actuator disk model. In order to analyse the radial load variation along the blades, the angular momentum being imparted to the wake by the propeller must be considered.

2.1.1 Effects of Wake Rotation

The conservation of angular momentum necessitates rotation of the slip-stream if the propeller is to impart useful torque. Jonkman [4] describes how the Rankine-Froude actuator disk model may be modified to account for this rotation. As such, assumptions 4) and 5) from the actuator disk model may be relaxed and three supplementary assumptions added:

1. The flow entering the control volume far upstream remains purely axial and uniform
2. The slip-stream can be split into a series of non-interacting, annular stream-tube control volumes
3. The angular velocity of the slip-stream flow far downstream of the propeller is low so the static pressure can be assumed to be the unobstructed ambient static pressure.

Although wake rotation is now included in the analysis, the assumption that the flow is irrotational has not been lifted. Conserving angular momentum about an axis consistent with the slip-stream's axis of symmetry can be applied to determine the torque.

$$Q = \frac{dL}{dt} = \frac{dI\omega}{dt} = \frac{dm}{dt}\omega r^2 \tag{1.8}$$

2.2 Blade Element Theory

Unless some state of flow is assumed, momentum theory does not provide enough equations to solve for the differential propeller thrust and torque at a given span location. Additional equations [1], [5] governing the state of the flow are dependent on the characteristics of the propeller blades, such as airfoil shape and twist distribution. Blade Element (BE) theory uses these geometrical properties to determine the forces exerted by a propeller on the flow-field.

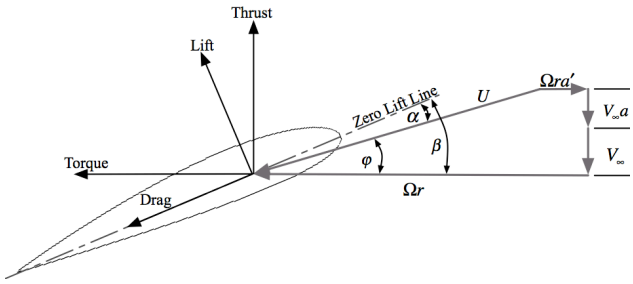

Fig. 2: Blade element aerodynamic forces

As the word *element* in the title suggests, BE theory, again, uses several annular stream-tube control volumes. At the propeller plane, the boundaries of these control volumes effectively split the blade into a number of distinct elements, each of width dr. At each element, blade geometry and flow-field properties can be related to a differential propeller thrust, dT, and torque, dQ, if the following assumptions are made:

1. Just as the annular stream-tube control volumes used in the slip-stream rotation analysis were assumed to be non-interacting [assumption (1)], it is assumed that there is no interaction between the analyses of each blade element
2. The forces exerted on the blade elements by the flow stream are determined solely by the two-dimensional lift and drag characteristics of the blade element airfoil shape and orientation relative to the incoming flow.

As we are required to obtain the local angle-of-attack to determine the aerodynamic forces on a blade element, we must first determine the inflow angle based on the two components of the local velocity vector.

$$\tan\varphi = \frac{V_\infty(1+a)}{\Omega r(1-a')} \tag{2.1}$$

From Fig. 2 the following relation is apparent,

$$U = \frac{V_\infty(1+a)}{\sin\varphi} \quad (2.2)$$

The induced velocity components in Equations (2.1) and (2.2) are a function of the forces on the blades and *blade element momentum* theory is used to calculate them. From Fig. 2, the thrust distributed around an annulus of width *dr* is equivalent to,

$$dT = \frac{1}{2}B\rho U^2(C_L\cos\varphi - C_D\sin\varphi)cdr \quad (2.3)$$

and the torque introduced by each annular section is given by,

$$dQ = \frac{1}{2}BpU^2(C_L\sin\varphi + C_D\cos\varphi)crdr \quad (2.4)$$

2.3 Blade Element Momentum Theory

Combining the results of the previous two analyses enables a model of the performance of a propeller whose airfoil properties, size, and twist distribution are known. This analysis is based on the differential propeller thrust, *dT*, and torque, *dQ*, derived from momentum theory and blade element theory, being equivalent.

Equations (2.3) and (2.4) are made more useful by noting that φ and *U* can be expressed in terms of induction factors etc [3], [6]. Substituting Equation (2.2) and carrying out some algebra,

$$dT = \sigma'\pi\rho\frac{V_\infty^2(1+a)^2}{\sin^2\varphi}\left(C_L\cos\varphi - C_D\sin\varphi\right)rdr \quad (3.1)$$

$$dQ = \sigma'\pi\rho\frac{V_\infty^2(1+a)^2}{\sin^2\varphi}\left(C_L\sin\varphi + C_D\cos\varphi\right)r^2dr \quad (3.2)$$

2.3.1. Prandtl Loss Correction

The effect on induced velocity in the propeller plane is most pronounced near the tips of the blades. The original blade element momentum theory does not consider the influence of vortices shed from the blade tips into the slip-stream on the induced velocity field. These tip-vortices create multiple helical structures in the wake, (as seen in Fig. 3), and play a major role in the induced velocity distribution along the propeller. To compensate for this deficiency in BEM theory, a tip-loss (or correction) factor, *F*, originally developed by Prandtl [7] is used.

As a blade has a suction-surface and a pressure-surface, air tends to flow over the blade tip from the lower (pressure) surface to the upper (suction) surface, effectively reducing the resulting forces in the vicinity of the tip. This theory is summarized by a correction to the induced velocity field and can be expressed simply by the following:

$$F = \frac{2}{\pi}\cos^{-1}e^{-f} \quad (3.3)$$

where,

$$f_{tip} = \frac{B}{2}\frac{R-r}{r\sin\varphi} \quad (3.4)$$

Much like the tip-loss model, the hub-loss model serves to correct the induced velocity resulting from a vortex being shed near the hub of the propeller. The model uses a similar implementation to that of the tip-loss to describe the effect of this vortex, replacing Equation (3.4) with,

$$f_{hub} = \frac{B}{2}\frac{r-R_{hub}}{r\sin\varphi} \quad (3.5)$$

For a given element, the local aerodynamics may be affected by both the tip- and hub-loss, in which case the two correction factors are multiplied to create the total loss factor.

Now, to relate the induced velocities in the propeller plane to the elemental forces of Equations (3.1) and (3.2), the conservation of momentum in the axial direction (between the far upstream and the far downstream section) must be considered. This states that the thrust introduced by each propeller annulus is equivalent to the change in axial momentum flow rate. The correction factor is used to modify the momentum segment of the BEM equations. From Equations (1.3), (1.4), and (1.7) , considering a radial differential,

$$dT = 4\pi r\rho V_\infty^2(1+a)aFdr \quad (3.6)$$

Considering a radial differential of Equation (1.8) and substituting Equation (1.6),

$$dQ = 4\pi r^3 \rho V_\infty \Omega(1+a)a' F dr \qquad (3.7)$$

Equalising Equations (3.6) and (3.7) with Equations (2.3) and (2.4), respectively, it is possible to obtain,

$$a = \left[\frac{4F\sin^2\varphi}{\sigma(C_L\cos\varphi - C_D\sin\varphi)} - 1 \right]^{-1} \qquad (3.8)$$

$$a' = \left[\frac{4F\sin\varphi\cos\varphi}{\sigma(C_L\sin\varphi - C_D\cos\varphi)} + 1 \right]^{-1} \qquad (3.9)$$

Thus, when we include two-dimensional airfoil tables of lift and drag coefficient as a function of the angle-of-attack, α, we have a set of equations that can be iteratively solved for the induced velocities and the forces on each blade element.

2.4 Vortex Structure of the Wake

Propeller theory generally presumes that, after an initial distortion, the vortex sheets shed from the trailing edges of the propeller blades form a set of interleaved helicoidal sheets which propagate uniformly downstream parallel to the slip-stream axis without further deformation as if they were rigid surfaces. In reality, these sheets will soon roll up into a set of helical vortex filaments and a central vortex filament of opposite sense on the axis.

The helicoidal vortex sheets are floating freely in an irrotational field with equal velocity on either side of the sheet, hence equal pressure. There is also no discontinuity of normal velocity, only a discontinuity of tangential velocity with magnitude equivalent to the vortex strength of the sheet.

Since there is no pressure discontinuity across the sheets, we deduce that sheets move axially backward without deformation. To approximate this we assume that the discrete bound vorticity is transformed in the slip-stream onto the surface of a vortex tube. There will be two components of this vorticity: a tube of elemental annular vortices that account for the thrust, and lines of elemental axial velocity along the tube that account for swirl [8].

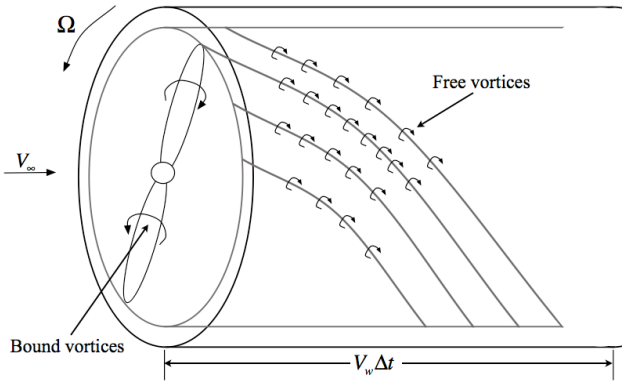

Fig. 3: Vortex tube

Only the annular vorticity is considered initially. This has strength, γ, and has to meet certain compatibility conditions:

1. The total pressure inside the wake is taken to be higher than the free-stream by the loading on the propeller. However, the inner and outer flows must have the same static pressure, which yields the condition,
$$\frac{1}{2}\rho V_s^2 = \frac{1}{2}\rho V_\infty^2 + \frac{T}{\pi R^2} \qquad (4.1)$$
2. From a consideration of the continuity of mass, the radius of the fully-developed slip-stream, R_s, is related to that of the propeller, R, by,
$$VR^2 = V_s R_s^2 \qquad (4.2)$$
3. By considering vorticity, the velocity jump across the wake boundary,
$$\gamma = V_s - V_\infty \qquad (4.3)$$

2.4.1. The Propeller related to the Vortex Wake

From the previous description of air flowing from the aerodynamic pressure side to aerodynamic suction, this is now described with the trailing vorticity which includes a reduction of the inflow angle towards the blade tip and, resultantly, a reduction in blade lift [10].

The induced velocity may be considered to be the resultant velocity at a point due to the entire system of bound and free vorticity. For simplicity we assume that the propeller blades are narrow and are distributed along equally spaced radial lines. Considerations of symmetry further reveal that equally spaced radial vortex

lines of equal strength induce no overall velocity on any one of the lines. These conditions therefore satisfy that the effect on each blade due to bound vorticity on the other blades can be ignored and only trailing vorticity contributes to the resultant velocity at a blade.

The fundamental expressions for the forces developed by the propeller may be described most conveniently by applying the Kutta-Joukowsky theorem,

$$dL = \rho U \times \Gamma dr \tag{4.4}$$

The cross-product relationship can be used to separate the two components of the resultant force, the thrust and the torque.

$$dT = \rho \Gamma \Omega r(1-a')dr \tag{4.5}$$

$$dQ = \rho \Gamma V_{\infty}(1+a)rdr \tag{4.6}$$

2.4.2. The Propeller Slip-stream

The deflection of the wake is determined by relating the propeller forces to the characteristics of the fully-developed slipstream. The aerodynamic forces generated by a propeller under any deviation from uniform flight parallel to the thrust axis will lead to deflection of the slip-stream.

We begin by considering the swirl component in the wake, represented by the vorticity γ_s. The axial component of the bound vorticity shed from the tip of the propeller blades per unit time is related to elemental axial vorticity lines along the stream-tube by,

$$B\Gamma V \Delta t = \gamma_s 2\pi R_s V \Delta t \tag{4.7}$$

so that,

$$2\pi R_s \gamma_s = B\Gamma \tag{4.8}$$

This satisfies the condition that the total vorticity shed at the tips, $B\Gamma$, must also be shed in the opposite sense at the roots as a discrete vortex down the axis.

Behind the propeller the vortex tube translates downstream as it is embedded between the inner and outer flows with a velocity, V_w. The annular component of the bound vorticity shed per unit time is related to the elemental annular vorticity distributed over the surface of the tube by,

$$\gamma 2\pi V_w = B\Gamma\Omega \tag{4.9}$$

But from a simplification of Equation (4.5), integrated across the blade, and for a number of blades, B,

$$B\Gamma\Omega = \frac{2T}{\rho R^2} \tag{4.10}$$

such that,

$$\rho\gamma V_w = \frac{T}{\pi R^2} \tag{4.11}$$

This combined vortex model, ensures that the swirl is contained within the stream-tube and induces no flow outside the wake [9].

2.4.3. Propeller at Incidence

We now consider a propeller at incidence to the slip-stream axis. In general, this will generate thrust and a tangential in-plane force N. Initially, thrust alone is considered; the inclusion of the in-plane force will follow as an incremental effect. Relative to the slip-stream, the down-going blade will have a forward velocity component, whereas the up-going side will be retreating.

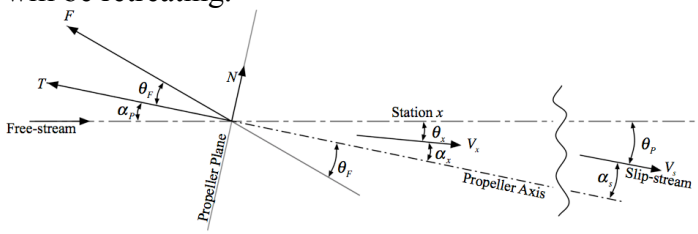

Fig. 4: Propeller slip-stream

Considering a simple propeller blade at a rotation angle ϕ (where $\phi = 0$ is at the top) with constant bound vorticity shed at the tip, the in-plane force acting normal to the blade will be $\rho\Gamma VR$ (for $\alpha_p = 0$). Taking an angular position ϕ around the propeller disk, the vertical component of the tip velocity is $\Omega R_s \sin(\phi)$, and the forward component of this is $\Omega R_s \alpha_s \sin(\phi)$ for small α_s. Equation (4.7) now becomes,

$$B\Gamma[V + \Omega R_s \alpha_s \sin(\phi)]\Delta t = \gamma_s 2\pi R_s V \Delta t \tag{4.12}$$

from which,

$$2\pi R_s \gamma_s = B\Gamma\left[\frac{1+\Omega R_s \alpha_s \sin(\phi)}{V}\right] \tag{4.13}$$

Compared with Equation (4.8), this shows an incremental sinusoidal variation of swirl velocity that will induce a downwash. Now a

sinusoidal vorticity distribution of the form $\gamma_0\sin(\phi)$ induces a uniform downwash of strength $\gamma_0/2$ inside the wake, which governs the deflection angle of the wake as it is counterbalanced by the up wash from the free-stream, $V_\infty\theta_p$.

From Equation (4.13), with $\phi = \pi/2$, $\gamma_0 = B\Gamma\Omega\alpha_s / (2\pi V)$, so that

$$V_\infty\theta_p = \frac{\gamma_0}{2} = \frac{B\Gamma\Omega\alpha_s}{4\pi V} \tag{4.14}$$

From Equation (4.10) we deduce that,

$$V_\infty\theta_p = \frac{T\alpha_s}{2\rho\pi R^2 V} \tag{4.15}$$

From Fig. 4, $\alpha s = \alpha p - \theta p$. Considering this along with Equation (1.1),

$$T\alpha_p = \rho\pi R^2 V(V_s + V_\infty)\theta_p \tag{4.16}$$

Where $T\alpha_p$ is the tangential component of thrust and must be equivalent to the tangential momentum flux in the slip-stream, which is represented by $\rho\pi R^2 V V_s\theta_p$ and resolved through θ_p. The other term, $\rho\pi R^2 V V_\infty\theta_p$, can be re-written, from Equation (4.2), as $\rho\pi R_s^2 V_s V_\infty\theta_p$, and represents the momentum flux of the part of the free-stream displaced by the cylindrical wake.

From the above it can be shown that

$$\frac{\theta_p}{\alpha_p} = 1 - \frac{V_\infty}{V} = \frac{C_T}{\left(1+\sqrt{1-C_T}\right)^2} \tag{4.17}$$

When $\alpha_p \neq 0$, to account for the net normal force it is assumed that, in addition to any constant bound vorticity that may be present to generate thrust, there is a component of bound vorticity that varies sinusoidally around the propeller disk, $\Gamma = \Gamma_0\sin(\phi)$. The effect on the slip-stream by the tangential in-plane force may be determined by resolving the normal-to-blade force vertically,

$$N(\phi) = \rho V R\Gamma_0 \sin^2(\phi) \tag{4.18}$$

Integration around the propeller disk, allowing for the number of blades, B, gives an average of

$$N = \frac{1}{2}\rho V B R\Gamma_0 \tag{4.19}$$

Following the analysis above, this is dispersed over the trailing wake stream0tube with a form $\gamma = \gamma_0\sin(\phi)$, where, from Equation (4.8),

$$2\pi R_s\gamma_0 = B\Gamma_0 \tag{4.20}$$

This will add to the downwash in the wake, balanced by the up wash from the free-stream, $V_\infty\theta p$ as above. The incremental effect is therefore,

$$\Delta V_\infty\theta_p = \frac{N}{2\pi\rho R R_s V} \tag{4.21}$$

Expressing the above equation in terms of the force coefficient and the propeller incidence, α_p, and adding this to the right hand side of Equation (4.15), the analysis proceeds until Equation (4.17) becomes,

$$\frac{\theta_p}{\alpha_p} = \left(1 - \frac{V_\infty}{V}\right) + \frac{1}{4}\frac{dC_N}{d\alpha_p}\frac{V_s^2}{V^2} \tag{4.22}$$

But, from actuator theory,

$$\frac{V_s^2}{V^2} = \frac{4V_s^2}{\left(V_s + V_\infty\right)^2} = \frac{4}{\left(1 + \frac{V_\infty}{V_s}\right)^2} \tag{4.23}$$

The incremental term due to the in-plane force now has a similar form to the contribution from thrust alone, and Equation (4.17) becomes [9],

$$\frac{\theta_p}{\alpha_p} = \frac{C_T + dC_N / d\alpha_p}{\left(1+\sqrt{1-C_T}\right)^2} \tag{4.24}$$

2.4.4. Slip-stream Trajectory

The trajectory of the slip-stream, and hence it's lateral displacement at any streamwise station, is governed by it's angle to the thrust line (or free-stream). The deflection from the datum can then be obtained by integration. The incidence case is considered and all angles are assumed small.

The approach adopted is to consider momentum in a direction perpendicular to the resultant force F, see Fig. 4 [10]. In this direction there is no force and the momentum must remain constant.

For a segment of slip-stream at station x downstream of the propeller, the longitudinal moment is $\rho S_x V_x dx$, and the tangential momentum due to the outer flow is $(\rho S_x V_\infty dx)\theta_x$. Momentum is constant along the normal to F, such that

$$\begin{aligned}&\rho S_x dx[V_x(\alpha_x+\theta_F)+V_\infty\theta_x]=\\&\rho S_s dx[V_s(\alpha_s+\theta_F)+V_\infty\theta_p]\end{aligned} \tag{4.25}$$

where the conditions on the right are those in the fully-developed slip-stream.

Writing $S_x = \pi R_x^2$, $S_s = \pi R_s^2$ and $S = \pi R^2$,

$$S_x V_x = S_s V_s = SV \tag{4.26}$$

and

$$\begin{aligned}&\rho S_p V dx\left[\left(\alpha_x+\theta_F\right)+\frac{V_\infty}{V_x}\theta_x\right]=\\&\rho S_p V dx\left[\left(\alpha_s+\theta_F\right)+\frac{V_\infty}{V}\theta_p\right]\end{aligned} \tag{4.27}$$

Now, $\theta_x = \alpha_p - \alpha_s$ and $\theta_p = \alpha_p - \alpha_s$, so that

$$\alpha_x\left(1-\frac{V_\infty}{V_x}\right)+\frac{V_\infty}{V_x}\alpha_p=\alpha_s\left(1-\frac{V_\infty}{V_s}\right)+\frac{V_\infty}{V_s}\alpha_p \tag{4.28}$$

From the equations of motion the streamwise distribution of velocity in the slip-stream is derived in [11] as,

$$\frac{V_s}{V_\infty}=1+s \tag{4.29}$$

in which

$$s=a\left[1+\frac{x}{\sqrt{x^2+d^2/4}}\right] \tag{4.30}$$

Equations (4.29) and (4.30) can be re-arranged to give

$$\frac{V_x}{V_s}=\frac{V_\infty}{V_s}+\left(1-\frac{V_\infty}{V_s}\right)f(x) \tag{4.31}$$

where

$$f(x)=\frac{1}{2}\left(1+\frac{x/D}{\sqrt{1/4+\left(\frac{x}{D}\right)^2}}\right) \tag{4.32}$$

Equation (4.28) can be re-written as

$$\alpha_x(V_x-V_\infty)V_s=\alpha_s(V_s-V_\infty)V_x+(V_x-V_s)V_\infty\alpha_p \tag{4.33}$$

and from Equation (4.31)

$$V_x-V_\infty=(V_s-V_\infty)f(x) \tag{4.34}$$

So finally,

$$\begin{aligned}&\frac{\alpha_x}{\alpha_p}=\frac{\alpha_s}{\alpha_p}\frac{1}{f(x)}\frac{V_x}{V_s}-\frac{V_\infty}{V_s}\left(\frac{1}{f(x)}-1\right)=\\&\frac{\alpha_s}{\alpha_p}\left[1+\frac{V_\infty}{V_s}\left(\frac{1}{f(x)}-1\right)\right]-\frac{V_\infty}{V_s}\left(\frac{1}{f(x)}-1\right)\end{aligned} \tag{4.35}$$

The diameter of the slip-stream at any station x is given by

$$\frac{D_x}{D}=\sqrt{\frac{1+a}{1+s}} \tag{4.36}$$

In order to calculate the displacement, z, of the slip-stream it is only necessary to integrate the angular deflection.

$$z=D\int_0^x \alpha_x\,dx \tag{4.37}$$

3. References

[1] Froude RE. *Trans Inst Naval Architects*, 1889;30:390.

[2] Rankine WJM. On the mechanical principles of the action of propellers. *Trans Inst Naval Architects (British)*, 1865;6(13).

[3] Glauert H. Airplane Propellers, vol iv, div. L. *In: Durand WF, editor. Aerodynamic Theory. Berlin: Julius Springer*, 1935 [Reprinted 1963 by Dover Publications, Inc., New York].

[4] Jonkman JM. Modeling of the UAE Wind Turbine for Refinement of FAST_AD. *NREL Technical Report* [NREL/TP-500-34755], 2003.

[5] Drzewiecki S. *Bulletin de L'Association Technique Maritime, Paris*. A Second Paper in 1901, 1892.

[6] Betz A. with Appendix by L. Prandtl, 1919, Schraubenpropeller mit Geringstem Energieverlust, Göttinger Nachrichten, Göttingen, p. 193-217. Reprinted in *Vier Abhandlungen uber Hydro- und Aerodynamik, L. Prandtl & A. betz,* 1927

[7] Wald QR. The distribution of circulation on propellers with finite hubs. *ASME Paper 64-WA/UNT-4*, Winter Annual Meeting, New York, 1964.

[8] Wald QR. The aerodynamics of propellers. *Progress in Aerospace Sciences 42, pg 85-128*, 2006.

[9] ESDU. Propeller slipstream modeling for incidence and sideslip. Item No. 06013, *Engineering Sciences Data Unit, London*, 2006.

[10] ESDU. Introduction to installation effects on thrust and drag for propeller-driven aircraft. Item No. 85015, *Engineering Sciences Data Unit, London*, 1985.

Contact Author

nasi@me.com; +27 83 324 2097

Copyright Statement